THE
PHYSICAL REVIEW

A journal of experimental and theoretical physics established by E. L. Nichols in 1893

SECOND SERIES, VOL. 156, NO. 2 10 APRIL 1967

Selective Excitation and Decay of Er^{3+} Fluorescence in LaF_3†

M. J. WEBER
Raytheon Research Division, Waltham, Massachusetts
(Received 9 November 1966)

A simple treatment of pulsed and steady-state selective-excitation experiments in multilevel systems is given and used to interpret the fluorescence excitation and decay properties of Er^{3+} in LaF_3. Fluorescence from eight different excited states was studied. From excitation spectra and pulsed selective excitation, decay modes were established involving level-by-level nonradiative cascade, arising from multiphonon emission, and level-bypassing radiative transitions. Energy transfer due to ion-ion interactions was deliberately avoided. Using pulsed-excitation techniques, multiexponential time-dependent fluorescences were observed and used to determine the lifetimes of all excited states below 40 000 cm^{-1}. In general, the smaller the energy gap to the next lower level, the shorter the lifetime, reflecting the dependence of the rate of multiphonon emission on the proximity of other levels. Fluorescence in LaF_3 is usually not detected when the energy gap is <1600 cm^{-1}. Fluorescence lifetimes were also measured as a function of temperature from 77 to ~700°K. Thermal quenching of the fluorescent properties is correlated with the increased importance of nonradiative transitions at higher temperatures.

INTRODUCTION

THE excitation and decay modes within a multilevel system, as exemplified by the optical energy levels of rare-earth ions, can be complex when many levels are involved and competing radiative and nonradiative transitions are present. Few detailed studies have been made of the rates and relative importance of various radiative and nonradiative processes active for excited paramagnetic-ion impurities in solids and their dependences upon the properties of the particular ion and host lattice. An understanding of these processes and the ability to make meaningful predictions and estimates thereof are of obvious importance when considering such systems for quantum-electronic applications. To obtain information about the modes and rates of radiative and nonradiative processes for rare-earth ions in crystals, an investigation was made of Er^{3+} in LaF_3.

Of the rare earths, Er^{3+} was chosen for study because its lower energy levels ($<40\,000$ cm^{-1}) are well established; in most crystals there are several fluorescing levels from which transitions occur involving a wide range of energies and between states of different character, and thus it offers sufficient variety and complexity to provide an adequate test of any theory or treatment of radiative and nonradiative processes. The spectroscopic properties of Er^{3+} in many host lattices have been reported[1] and are particularly well known in LaF_3 from the work of Krupke and Gruber.[2] Pollack[3] has made an extensive study of the spectra and decay properties of Er^{3+} in CaF_2, however detailed interpretation of the results is hampered by the existence of several types of charge-compensated lattice sites.[4] Fluorescence lifetimes of several Er^{3+} levels in various crystals have been reported by Barasch and Dieke.[5]

The experimental approach used to unravel the modes of energy decay within a complex multilevel system such as Er^{3+} is one of selective excitation and observation wherein monochromatic radiation is applied to excite ions into chosen energy levels and the fluorescence is observed from particular lower levels. A combination of steady-state fluorescence and excitation spectra and pulsed selective excitation experiments were used. The

† Research supported in part by U. S. Army Engineering Research and Development Laboratory, Fort Belvoir, Virginia, under Contract No. DA44-009-AMC-743(T).

[1] See, for example, G. H. Dieke, in *Advances in Quantum Electronics*, edited by J. Singer (Columbia University Press, New York, 1963), p. 237 and references therein.
[2] W. F. Krupke and J. B. Gruber, J. Chem. Phys. **39**, 1024 (1963); **41**, 1225 (1964); **42**, 1134 (1965).
[3] S. A. Pollack, J. Chem. Phys. **38**, 2521 (1963); **40**, 2751 (1964).
[4] C. W. Rector, B. C. Pandey, and H. W. Moos, J. Chem. Phys. **45**, 171 (1966).
[5] G. E. Barasch and G. H. Dieke, J. Chem. Phys. **43**, 988 (1965).

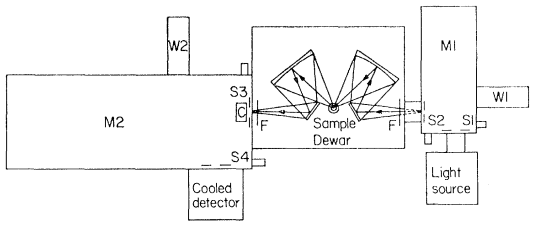

FIG. 1. Block diagram of apparatus for selective excitation and fluorescence studies. M1—grating monochromator $f/4.4$, 66 Å/mm; M2—grating monochromator $f/4.4$, 33 Å/mm; light sources—Osram XBO-900, Tungsten DKM, FX-12 flashtube; detectors—1P28, 7102, and 7265 photomultipliers, Ektron PbS; W1, W2—wavelength dial, motor driven scan; S1, S2, S3, S4—adjustable slits; F—filters; C—light chopper.

time-dependent fluorescence from a multilevel system following pulsed selective excitation consists in general of a linear combination of exponential terms. From an analysis of the transient behavior, using solutions of the rate equations for simple multilevel systems, the decay modes and lifetimes of both fluorescent and nonfluorescent levels can be determined. The lifetimes also reveal which levels are important for the energy cascade, and which are the bottlenecks in the process.

The lifetime of an excited state is a measure of a combination of all probabilities for radiative and nonradiative decay. In this paper we shall be interested principally in elucidating the various operative modes of excitation and decay and determining their relative importance; in a second paper[6] (referred to hereafter as II) the questions of the individual rates of radiative and nonradiative transitions, quantum efficiencies, and their dependence upon the energy and eigenstates involved are examined.

Radiative processes, as used herein, include purely electronic or zero-phonon transitions and phonon-assisted radiative transitions. Nonradiative processes include single- and multiple-phonon emission, resonant or phonon-assisted energy transfer arising from ion-ion coupling, or other energy-exchange mechanisms. For rare-earth concentrations of $\gtrsim 1\%$ in LaF_3, ion-ion interactions are evident from changes in the optical spectra, fluorescence lifetimes,[7] and in energy transfer experiments.[8] Since our ultimate interest is the investigation of multiphonon nonradiative processes, an attempt was made to minimize the above effects by using crystals containing relatively low rare-earth concentrations.

EXPERIMENTAL

The apparatus and experimental arrangement used for the selective excitation and observation of steady-state and transient fluorescence are depicted schematically in Fig. 1. The system has all mirror optics and emphasizes high speed rather than resolution. For recording steady-state excitation and fluorescence spectra, tungsten or high-pressure xenon arc lamps were used. The fluorescence was modulated by a tuning-fork light chopper and the signal integrated and recorded using phase-sensitive detection techniques.

Fluorescence decay processes were investigated by exciting the sample with a light pulse from a xenon flashtube and displaying the detector output on an oscilloscope. Lifetimes $\gtrsim 3$ μsec were measurable with the present apparatus. When the sample fluorescence was too weak to be observed and measured directly from an oscilloscope presentation, the signal-to-noise-ratio was improved by repetitively pulsing the system and using gated-integration techniques.[9] A small portion of the transient signal was sampled, integrated, and the output displayed on a chart recorder. By progressively varying the time interval between the excitation pulse and the sampling pulse, the transient decay was plotted. Time-resolved excitation and fluorescence spectra can be recorded by selecting a fixed sampling time and duration and then scanning the appropriate monochromator.

An alternative method for improving the signal-to-noise ratio of weak transient fluorescence was digital signal averaging using an on-line computer (Technical Measurements Corporation Model CAT-1024). In this instrument the signal is divided and summed in up to 1024 separate channels, the signal-to-noise improvement being proportional to the square root of the number of signals added. Since the minimum sampling interval per channel was 20 μsec, this approach was limited to measurements of the longer decay times.

To record the transient fluorescence signals, the detector or CAT-1024 output was displayed on an oscilloscope and photographed. The characteristic $1/e$ lifetime for a simple exponential decay was measured either directly from the photograph or from a semilog plot of the time dependence. A rapid measurement of the decay time was obtained by applying an exponentially varying voltage to the horizontal input of the oscilloscope. The decay time of this exponential sweep was calibrated and variable over four decades, thus by adjusting it until a straight line was observed on the oscilloscope, the lifetime of the fluorescence signal was determined. Any departure from a single exponential decay was also evident.

The fluorescent samples were doped single crystals grown by Optovac, Inc. and were typically a few mm on a side. They were suspended in a long quartz Dewar open at both ends through which flowed dry nitrogen gas. This gas passed through a liquid-nitrogen heat exchanger and over a nichrome wire heater before reaching the sample. By adjusting the gas flow rate and the

[6] M. J. Weber, Phys. Rev. (to be published).
[7] See, for example, C. K. Asawa, and M. Robinson, Phys. Rev. **141**, 251 (1966).
[8] M. R. Brown, J. S. S. Whiting, and W. A. Shand, J. Chem. Phys. **43**, 1 (1965).
[9] The gated integrator was an adaptation of one described by R. J. Blume, Rev. Sci. Instr. **32**, 1016 (1961).

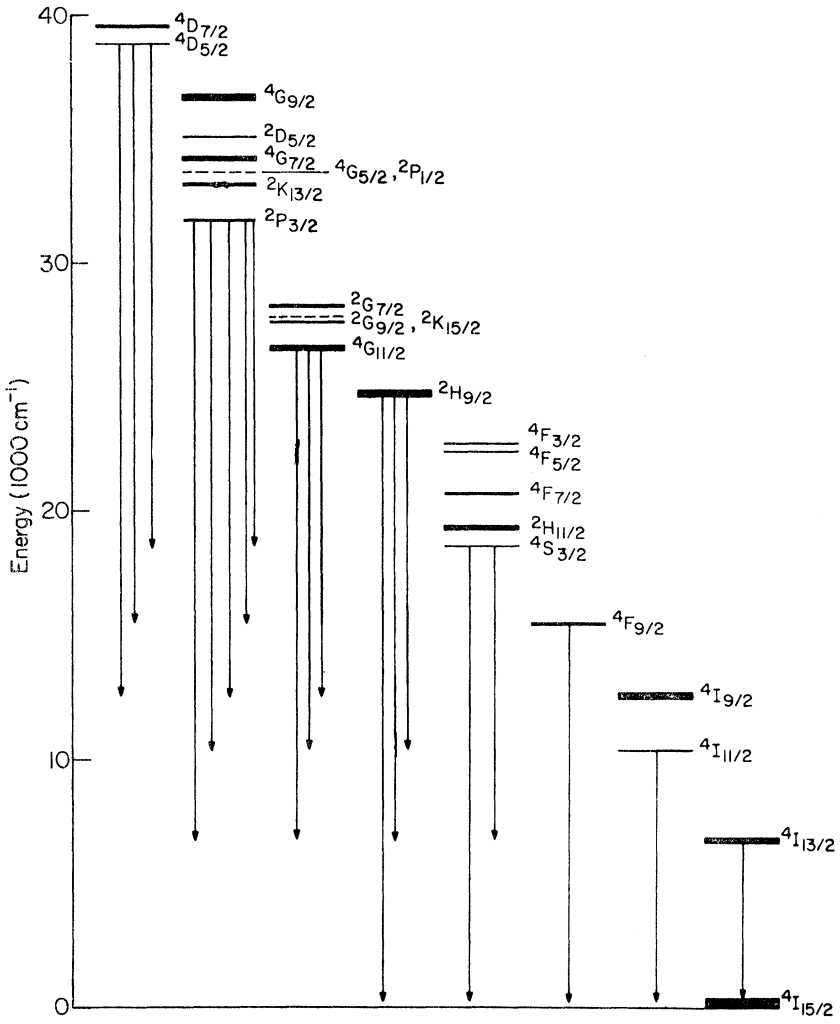

FIG. 2. Energy levels and fluorescence transitions of Er^{3+} in LaF_3.

power dissipation in the heater, the sample temperature could be varied quickly and continuously from approximately 77 to 800°K. The temperature was measured by thermocouples inserted into or alongside the sample.

ENERGY LEVELS AND FLUORESCENCE SPECTRUM

Trivalent Er has a $4f^{11}$ electronic configuration. Almost all of the expected energy levels of Er^{3+} in LaF_3 below 40 000 cm^{-1} have been identified in the absorption and fluorescence spectra studies of Krupke and Gruber[2] (KG). The observed location and ordering of the (SLJ) multiplets are shown in Fig. 2. (Throughout this paper the L and S labeling of states will correspond to that used by KG, that is, that of the LS-coupled state to which each intermediate coupled state reduces as the spin-orbit parameter is decreased to zero.) The predicted locations of levels which have thus far not been identified are denoted by dashed lines. In most cases the energy levels arising from the partial removal of the $(2J+1)$-fold degeneracies by the crystalline Stark field were measured by KG and, while not shown individually, the extent of the crystal-field splitting is indicated by the thickness of the levels.

Fluorescence has been observed from eight [SLJ] states. Krupke and Gruber reported fluorescence from $^4F_{9/2}$, $^4S_{3/2}$, $^2H_{9/2}$, $^2P_{3/2}$, and $^4D_{5/2}$ and stimulated emission from $^4I_{13/2}$ to an excited crystal-field level of $^4I_{15/2}$. We have observed fluorescence from all six of these levels and, in addition, from $^4I_{11/2}$ and $^4G_{11/2}$ and, at elevated temperatures, from thermally populated levels such as $^2H_{11/2}$. Some of the main fluorescence transitions from these eight metastable states which were observed and used in the course of these studies are shown in Fig. 2. No attempt was made to record all possible transitions, however.

Weak emission from other levels undoubtedly exists since radiative transitions are usually not strictly forbidden. Where the energy gap to the next lower level is small, the quantum efficiencies and fluorescence intensities are generally low. Very weak fluorescences were

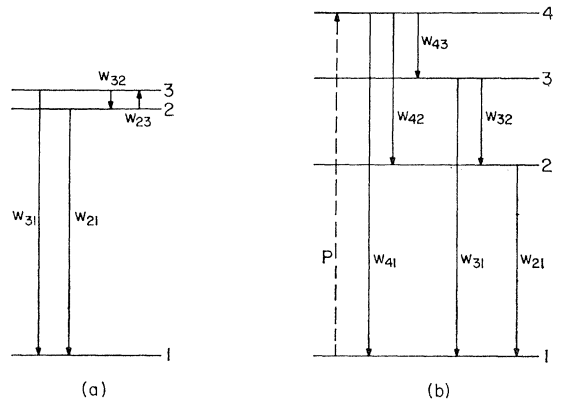

FIG. 3. Typical relaxation transitions of excited rare-earth ions for simple three- and four-level systems.

detected at 77°K which appeared to originate from $^4F_{5/2}$ and $^4I_{9/2}$ to $^4I_{15/2}$ but no useful measurements could be made.

A characteristic feature of fluorescence from rare-earth ions in crystals, which is evident from Fig. 2, is that emission is observed principally from those levels for which there is a comparatively large energy gap to the next-lower level. Fluorescence is not observed from closely spaced levels, such as those immediately above $^4S_{3/2}$, $^4G_{11/2}$, and $^2P_{3/2}$, because ions in these levels rapidly decay to the next-lower level by nonradiative transitions. As the energy gap becomes larger, the probability for these processes decreases and eventually fluorescence becomes a competitive mode of decay. In the present ion-lattice combination, this occurs for energy gaps >1600 cm^{-1}.

PULSED SELECTIVE EXCITATION

Theory

The time dependence of fluorescence signals following a short, intense pulse of monochromatic radiation applied to raise ions into selected excited states can be used to determine excited-state lifetimes and can provide a signature of the states limiting decay to the fluorescent level. Since the number of possible decay modes for a complex multilevel system can be quite large, we shall examine the transient behavior for a few simple cases which illustrate the essential features of decay modes frequently encountered for rare-earth ions in general and Er^{3+} in LaF_3 in particular. Throughout, treatment of transitions of the type arising from ion-ion coupling and resonant energy transfer[7] will be omitted.

Relaxation within a given crystal-field multiplet and between different crystal-field multiplets will be discussed separately. In the former, energy level separations typically range up to a few hundred cm^{-1}. This is usually within the fundamental frequency spectrum of lattice vibrations and hence one- and two-phonon relaxation processes are probable. From investigations of spin-lattice relaxation[10] within the ground-state multiplet, these processes are known to be rapid and lead to lifetime broadening of crystal-field components in optical spectra. The separations between crystal-field multiplets, on the other hand, range from several hundreds to thousands of cm^{-1}. Fluorescence is observed from multiplets having relatively large energy gaps to the next lower multiplet, the radiative decay times being in general very much longer than the intramultiplet relaxation times.

To examine the intramultiplet equilibration, consider the simple three-level system in Fig. 3(a) consisting of a terminal level 1 and two closely spaced levels 2 and 3 representing crystal-field levels of an excited fluorescing state. Assume the ions are initially excited into one or both of the upper states either directly from the ground state or by rapid cascade from higher excited states. The ions then relax by nonradiative transitions connecting levels 2 and 3 and by photon emission to level 1. The rate equations[11] for the level populations n_i are

$$\begin{bmatrix}\dot{n}_1\\ \dot{n}_2\\ \dot{n}_3\end{bmatrix}=\begin{bmatrix}0 & w_{21} & w_{31}\\ 0 & -(w_{21}+w_{23}) & w_{32}\\ 0 & w_{23} & -(w_{31}+w_{32})\end{bmatrix}\begin{bmatrix}n_1\\ n_2\\ n_3\end{bmatrix}. \quad (1)$$

The solutions of Eq. (1) at time t following the excitation are of the form

$$n_i(t)=A_ie^{m_+t}+B_ie^{m_-t}, \quad (2)$$

where

$$2m_\pm=-(w_{31}+w_{32}+w_{21}+w_{23}) \pm[(w_{31}+w_{32}-w_{21}-w_{23})^2+4w_{23}w_{32}]^{1/2}. \quad (3)$$

The coefficients A and B are determined by the initial values of n_i at $t=0$ and are related by

$$A_3=\left(\frac{w_{21}+w_{23}+m_+}{w_{32}}\right)A_2, \quad B_3=\left(\frac{w_{21}+w_{23}+m_-}{w_{32}}\right)B_2. \quad (4)$$

When the various decay rates in Eq. (3) are comparable, an explicit lifetime cannot be given for an individual level and the multiexponential time dependence in Eq. (2) must be considered.

The probabilities for nonradiative transitions between crystal-field levels are usually very much faster than radiative decay probabilities. Also, since they arise from thermal lattice modulation of the crystalline field, they are related from detailed balance considerations by $w_{32}/w_{23}=e^{E/kT}$, where E is the energy level separation.

[10] Spin-lattice relaxation of rare-earth ions in LaF_3 has been investigated by M. B. Schulz and C. D. Jeffries, Phys. Rev. **149**, 270 (1966).

[11] Radiation trapping is not considered in Eq. (1) because for the higher excited states of the rare earths, resonance radiation is frequently only one of many radiative transitions. The effects of trapping can be included, if desired, by introducing a multiplicative "escape factor" in the radiative probability to the ground state; this factor ranges from unity (corresponding to no trapping) to zero (for the radiation-trapped limit).

In these limits, the decay rates in Eq. (3) reduce to

$$m_+=(w_{21}+w_{31}e^{-E/kT})/(1+e^{-E/kT}). \quad (5a)$$

$$m_-=-(w_{32}+w_{23}), \quad (5b)$$

and

$$A_3\approx(w_{23}/w_{32})A_2=e^{-E/kT}A_2, \quad B_3\approx -B_2. \quad (6)$$

If N_e is the total number of ions initially excited into levels 2 and 3, then

$$n_2(t)=\frac{N_e}{1+e^{-E/kT}}(e^{m_+t}+e^{-E/KT}Be^{m_-t}),$$
$$n_3(t)=\frac{N_e e^{-E/kT}}{1+e^{-E/kT}}(e^{m_+t}-e^{m_-t}), \quad (7)$$

where $2B=n_2(0)-n_3(0)-N_e\tanh(E/2kT)$. The transient behavior thus consists of rapid thermalization of the ion population among the crystal-field levels in a characteristic time $(w_{32}+w_{23})^{-1}$ followed by decay to the ground state at a rate m_+ given by Eq. (5) This rapid intramultiplet equilibration commonly prevails except where low temperatures, crystal-field splittings large with respect to available phonon frequencies, or forbidden transitions render the approximations w_{32}, $w_{23}\gg w_{31}$, w_{21} invalid.

Assuming rapid thermalization of the level populations within a crystal-field multiplet, we now investigate the decay from the multiplet by treating it as an equivalent free-ion level. The types of decay modes which may occur between J multiplets are indicated in Fig. 3(b). This simplified, multilevel system will again suffice to illustrate the behavior observed for $LaF_3:Er^{3+}$ and can readily be extended. The transitions shown may arise from both radiative and nonradiative processes. The multiplet separations and the temperature are assumed to be such that the probabilities for upward transitions are negligible. The lifetime of a multiplet k is determined by a summation of all possible radiative and nonradiative probabilities given by

$$\frac{1}{\tau_k}=\sum_{i,j}Z_k^{-1}e^{-E_i/kT}w_{ij}\equiv W_k, \quad (8)$$

where Z_k is the partition function and the summation includes all levels i within multiplet k and all terminal levels j in other multiplets. In the high-temperature limit of equally populated crystal-field levels within multiplet k, Eq. (8) reduces to $(2J+1)^{-1}\sum_{i,j}w_{ij}$, which is essentially a free-ion type result.

The general time dependency of decay for an M-level system is composed of a linear combination of exponential terms of the form

$$n_m(t)=\sum_{k\geq m}^{M}A_k{}^m e^{-t/\tau_k}, \quad (9)$$

where τ_k is given by Eq. (8) and the $A_k{}^m$'s are determined by the initial conditions. The rate equations for the decay depicted in Fig. 3(b) are

$$\begin{bmatrix}\dot{n}_1\\ \dot{n}_2\\ \dot{n}_3\\ \dot{n}_4\end{bmatrix}=\begin{bmatrix}0 & W_2 & w_{31} & w_{41}\\ 0 & -W_2 & w_{32} & w_{42}\\ 0 & 0 & -W_3 & w_{43}\\ 0 & 0 & 0 & -W_4\end{bmatrix}\begin{bmatrix}n_1\\ n_2\\ n_3\\ n_4\end{bmatrix} \quad (10)$$

and have solutions

$$n_4(t)=n_4(0)e^{-W_4t}, \quad (11a)$$

$$n_3(t)=\left[n_3(0)+\frac{w_{43}n_4(0)}{W_4-W_3}\right]e^{-W_3t}-\frac{w_{43}n_4(0)}{W_4-W_3}e^{-W_4t}, \quad (11b)$$

$$n_2(t)=A_2{}^2e^{-W_2t}+A_3{}^2e^{-W_3t}+A_4{}^2e^{-W_4t}, \quad (11c)$$

where

$$A_4{}^2=\left[\frac{w_{43}w_{32}}{(W_4-W_3)(W_4-W_2)}-\frac{w_{42}}{W_4-W_2}\right]n_4(0),$$
$$A_3{}^2=-\frac{w_{32}n_3(0)}{W_3-W_2}-\frac{w_{43}w_{32}n_4(0)}{(W_4-W_3)(W_3-W_2)}, \quad (12)$$
$$A_2{}^2=n_2(0)-A_3{}^2-A_4{}^2.$$

Consider the case where ions are selectively excited into a single energy level such as 4, i.e., $n_4(0)=N_e$, $n_3(0)=n_2(0)=0$. The fluorescence from the level initially excited exhibits a simple exponential decay Eq. (11a). The time dependence of the fluorescence from the next lower level, however, is composed of the difference of two exponential terms, one corresponding to decay from level 4 into level 3 and the other the subsequent decay of level 3. The intensity will be a maximum at time

$$t_{\max}=[1/(W_4-W_3)]\ln(W_4/W_3). \quad (13)$$

The transient fluorescence from level 2 is more complicated, since it is populated by transitions from both levels 3 and 4. If the dominant decay is via a step-by-step cascade $4\rightarrow 3\rightarrow 2$, that is, $w_{42}\approx 0$, and if furthermore $W_3\gg W_2$, W_4, then the fluorescence from level 3 will always be weak because of the multiplicative factor $[w_{43}/(W_4-W_3)]\ll 1$ in Eq. (11b). Under the same conditions the fluorescence from level 2 is proportional to

$$\left[\frac{w_{43}}{W_4-W_2}-\frac{w_{43}}{W_3}\right]e^{-W_2t}+\frac{w_{43}}{W_3}e^{-W_3t}-\frac{w_{43}}{W_4-W_2}e^{-W_4t}. \quad (14)$$

If $W_4>W_2$, the growth of fluorescence in Eq. (14) is governed by the longer-lived of the higher excited states involved in the cascade. The rise time can therefore be used to identify the bottleneck in a level-by-level cascade.

Observations

Examples of the above decay modes were observed for excited states of Er^{3+} in LaF_3. Oscilloscope photographs

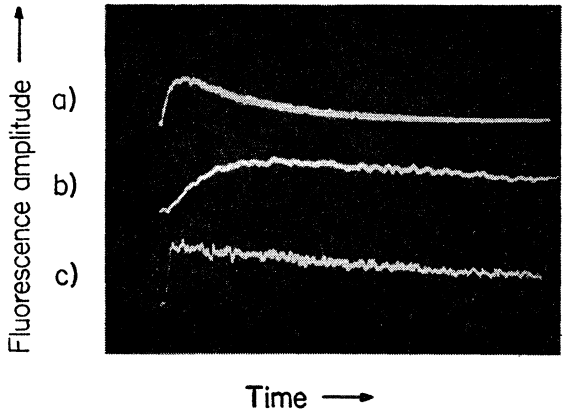

FIG. 4. Oscilloscope photograph of $^4S_{3/2}$ fluorescence at 77°K following pulsed excitation into (a) $^4G_{11/2}$, total sweep 5.0 msec, (b) $^4G_{11/2}$, total sweep 1.0 msec, (c) $^2H_{11/2}$, total sweep 1.0 msec.

of the transient fluorescence from $^4S_{3/2}$ are shown in Fig. 4. The top trace was generated by excitation into $^4G_{11/2}$. The initial rise, seen on the expanded scale of trace (b), and the subsequent decay are characteristic of the behavior predicted by Eq. (14) and correspond, respectively, to the lifetimes of $^2H_{9/2}$, which is the longest-lived state in the step-by-step cascade from $^4G_{11/2}$ to $^4S_{3/2}$, and $^4S_{3/2}$. When ions are excited into $^2H_{11/2}$, however, they rapidly decay to $^4S_{3/2}$ as evident by the absence of a measurable rise time in trace (c).

The effect of a long-lived excited state which bottlenecks energy cascade and limits the population buildup in a lower, shorter-lived state occurs in selective excitation experiments of the $^4G_{11/2}$ fluorescence. Intense fluorescence is observed when ions are excited into the $^4G_{11/2}$ to $^2G_{7/2}$ group of states since the excitation rapidly cascades to the $^4G_{11/2}$ metastable state. When ions are excited into $^2P_{3/2}$ or higher states, however, only very weak fluorescence is observed because the long-lived $^2P_{3/2}$ and $^4D_{5/2}$ states restrict the rate of energy cascade.

A more complicated situation involving both level-by-level cascade and level-bypassing transitions occurs in the excitation of the $^4F_{9/2}$ fluorescence. The transient behavior observed for two different excitation states and two different temperatures are shown in Fig. 5 (the data are from the analog output of the CAT-1024). Traces (a) and (b), taken at 77°K, show the signals derived from selective excitation into $^4G_{11/2}$ and $^2H_{11/2}$. Whereas in (b) a cascade $^2H_{11/2} \rightarrow {}^4S_{3/2} \rightarrow {}^4F_{9/2}$ occurs, in (a) part of the ions rapidly decay to $^4F_{9/2}$ bypassing $^4S_{3/2}$. This accounts for the fast buildup of the signal. Since the lifetime of $^4S_{3/2}$ is slightly longer than that of $^4F_{9/2}$, the longest time constant in these traces is characteristic of $^4S_{3/2}$ and not the fluorescent level. The over-all time dependence in (a) is describable by Eq. (11c). At higher temperatures, the $^4F_{9/2}$ transient fluorescences in traces (c) and (d) appear similar because now the dominant decay from $^4G_{11/2}$ to $^4F_{9/2}$ also occurs via a cascade which includes $^4S_{3/2}$.

In view of the $^4I_{9/2}$-$^4I_{11/2}$ energy gap, observation of fluorescence from $^4I_{9/2}$ might be expected, however, several difficulties are encountered when using pulsed excitation. Direct pumping of ions into $^4I_{9/2}$ was impractical because absorption into a single multiplet was small and the source radiation and $^4I_{9/2} \rightarrow {}^4I_{15/2}$ fluorescence were not well isolated. Excitation of $^4I_{9/2}$ via level-by-level cascade from above suffers because the $^4F_{9/2}$ lifetime is longer than that determined for $^4I_{9/2}$ and hence restricts population buildup in $^4I_{9/2}$. When excitation via direct radiative transitions from higher excited states is attempted, other fluorescences (such as $^2P_{3/2} \rightarrow {}^2H_{11/2}$ and $^2H_{9/2} \rightarrow {}^4I_{9/2}$) are excited which, due to similar wavelengths and lifetimes, tend to mask the sought-for fluorescence.

In Table I we list the lower energy levels of Er^{3+}, indicate from which levels fluorescence has been observed in LaF_3, and give the lifetimes discussed below. In the final column are noted those levels or groups of levels which are evident from the fluorescence rise time and/or transient behavior observed in pulsed experiments involving selective excitation into these levels.

EXCITED-STATE LIFETIMES

The lifetimes, or upper limit thereof, for all excited states of Er^{3+} in LaF_3 below 40 000 cm^{-1} were measured following pulsed excitation. For the eight levels which fluoresce strongly, the lifetimes were determined from the observed fluorescence decay. To avoid the necessity of unraveling multiexponential time dependences, the ions were excited directly into the level of interest whenever possible. The lifetimes of nonfluorescent levels were determined by observing the time dependence of the fluorescence from lower levels following pulsed selective excitation into the level of interest. From the initial rise time and/or the time of the intensity maximum, as described by Eqs. (11) and (13), the lifetimes were found. Frequently an undistorted rise was not observable because of the finite duration of the excitation pulse (typically a few microseconds) and hence only the upper

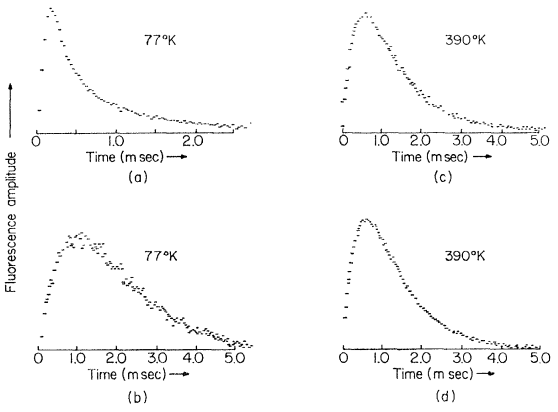

FIG. 5. Time dependence of the $^4F_{9/2}$ fluorescence following pulsed excitation into $^4G_{11/2}$ (a), (c) and $^2H_{11/2}$ (b), (d).

limits for the lifetimes are reported. For closely spaced energy levels, the actual lifetimes are undoubtedly very much shorter than the limiting value given. The lifetime results at liquid-nitrogen temperatures are summarized in Table I. The estimated errors range from $\approx 5\%$ for the strongest fluorescence lines to $\approx 20\%$ for the weakest.

The lifetimes given in Table I (and later in Fig. 6) are for a 0.095% Er sample, with the exception of the $^4D_{5/2}$ and $^4I_{13/2}$ lifetimes which were measured using a 0.42% Er sample. Concentration-dependent lifetimes have been reported for rare earths in LaF_3 by several investigators[7] and attributed to an enhanced probability for energy transfer via ion-ion coupling, the effects being particularly noticeable for concentrations $\gtrsim 1\%$. A comparison of the lifetimes of $^4I_{11/2}$, $^4F_{9/2}$, $^4S_{3/2}$, $^2H_{9/2}$, and $^2P_{3/2}$ measured at room temperature for crystals containing 0.095 and 0.42% Er revealed lifetime decreases of $<20\%$. Therefore any contributions to the lifetimes in Table I from energy transfer processes are believed to be small.

Lengthening of the observed lifetimes due to radiation trapping[12] should be a small effect for the higher excited states of Er because resonance radiation is only one of many possible radiative transitions. In the case of $^4I_{13/2}$, however, radiation trapping may be active. No significant $^4I_{13/2}$ lifetime difference was detected at room temperature for 0.095 and 0.42 Er crystals, but the weakness and multiexponential character of the signals gave rise to large experimental uncertainties, 25%.

The temperature dependences of the fluorescence lifetimes in the range from 77 to 700°K are shown in Fig. 6. Whereas at liquid-nitrogen temperatures the lifetimes exhibit little variation with temperature, they generally decrease monotonically with increasing temperature. Although a discussion of the temperature dependences is beyond the intended scope of this paper,

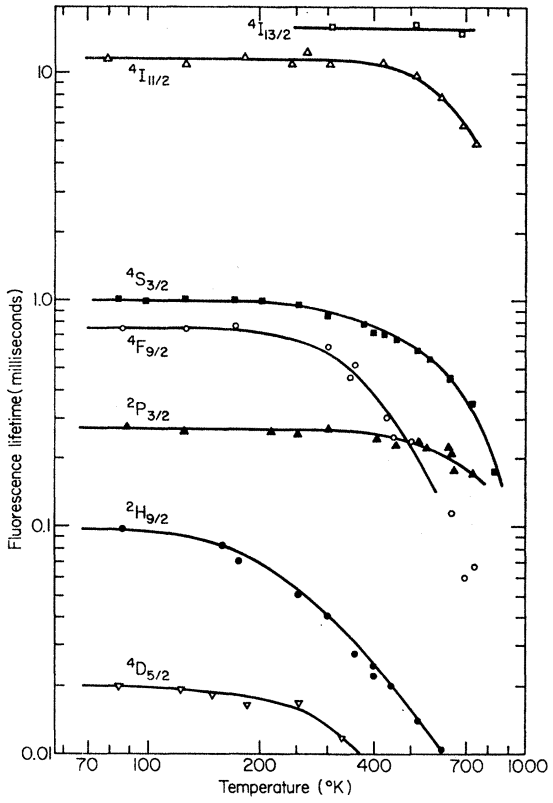

FIG. 6. Temperature dependences of the fluorescence lifetimes for Er^{3+} in LaF_3.

among the possible origins are (1) thermal population of levels having different decay probabilities and (2) the intrinsic temperature dependence of various transition probabilities. Levels thermally populated may be either other crystal-field levels of the fluorescing multiplet or levels of higher J multiplets. The resulting transient recovery, as discussed earlier in connection with the

TABLE I. Lifetimes and excitation modes of excited states of Er^{3+} in LaF_3.

Level	Fluorescence	Lifetime at 77°K (msec)	Excitation[e]
$^4I_{13/2}$	Yes[a]	13	$^4I_{11/2}$, $^4S_{3/2}$
$^4I_{11/2}$	Yes[a]	11	$^4I_{9/2}$, $^4F_{9/2}$, $^4S_{3/2}$, $^2P_{3/2}$, $^4D_{5/2}$
$^4I_{9/2}$	c	~ 0.15[d]	
$^4F_{9/2}$	Yes[a,b]	0.75	$^4S_{3/2}$, $^2H_{9/2}$-$^4G_{11/2}$, $^4D_{5/2}$
$^4S_{3/2}$	Yes[a,b]	1.0	$^2H_{11/2}$, $^4F_{5/2}$, $^2H_{9/2}$
$^2H_{11/2}$, $^4F_{7/2}$	No	<0.005[d]	
$^4F_{5/2}$, $^4F_{3/2}$	Very weak[a]	0.005-0.01[d]	
$^2H_{9/2}$	Yes[a,b]	0.095	$^4G_{11/2}$
$^4G_{11/2}$	Yes[a]	~ 0.003	$^2G_{9/2}$-$^2G_{7/2}$
$^2G_{9/2}$, $^2K_{15/2}$, $^2G_{7/2}$	No	<0.003[d]	
$^2P_{3/2}$	Yes[a,b]	0.29	$^2K_{13/2}$, $^4D_{5/2}$
$^2K_{13/2}$, $^4G_{5/2}$, $^4G_{7/2}$, $^2D_{5/2}$, $^4G_{9/2}$	No	<0.005[d]	
$^4D_{5/2}$	Yes[a,b]	0.020	$^4D_{5/2}$-$^4D_{7/2}$

[a] This paper.
[b] W. F. Krupke and G. B. Gruber, J. Chem. Phys. **41**, 1225 (1964).
[c] See discussion in text.
[d] Determined from the rise time of fluorescence from a lower level following pulsed excitation into this level.
[e] Excitation via these levels or groups of levels is evident from the observed rise time of the fluorescence following pulsed-selective excitation.

[12] M. J. Taylor and W. A. Shand, Brit. J. Appl. Phys. **17**, 141 (1966).

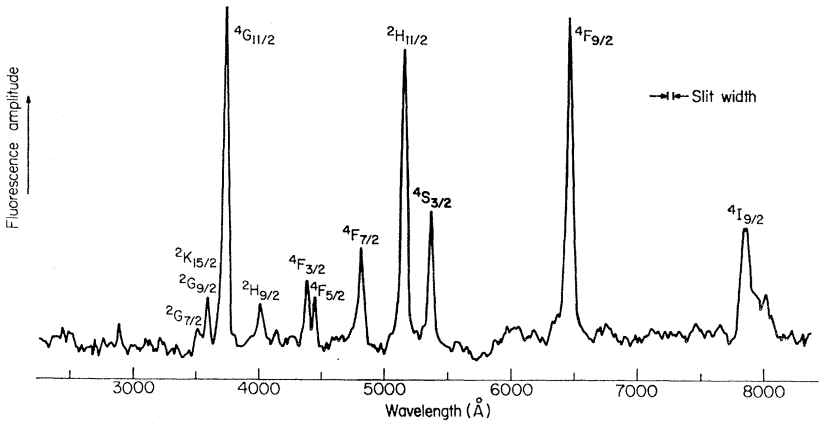

FIG. 7. Excitation spectrum of $^4I_{11/2}$ fluorescence at 78°K.

case in Fig. 3(a), may exhibit a nonexponential behavior and a net temperature-dependent relaxation rate of the type given in Eqs. (5a) and (8). As an example, the minimum $^4S_{3/2}$-$^2H_{11/2}$ level separation is 678 cm^{-1} and at elevated temperatures fluorescence from $^2H_{11/2}$ is observed. Since the $^2H_{11/2}$ radiative probability is greater than that of $^4S_{3/2}$ (see II), this leads to a shortening of the lifetime attributed to $^4S_{3/2}$. As for (2), if multiphonon nonradiative processes or phonon-assisted transitions are significant, their intrinsic temperature dependences will be reflected in the total lifetime. The rate of a n-phonon process varies from a constant at low temperature, corresponding to spontaneous emission of phonons, to a T^n dependence when $kT \gg E_{\text{phonon}}$. The fundamental phonon frequencies in LaF_3[13] range up to ≈ 400 cm^{-1} and therefore, assuming the higher-energy phonons made the most important contributions, the high-temperature limit is not reached in the present experiments. The number of phonons required to conserve energy in a nonradiative transition and hence the power of T in the high-temperature limit is, of course, dependent upon the size of the energy gap. Phonon-assisted radiative transitions which appear as weak sidebands of the zero-phonon lines for rare earths in LaF_3[14] may also make a nonnegligible, temperature-dependent contribution to the lifetimes at elevated temperatures.

EXCITATION SPECTRA

Theory

Fluorescence spectra reveal the presence of radiative transitions; excitation spectra, on the other hand, can reveal the existence of nonradiative transitions between levels. The presence or absence of levels in the excitation spectra can be used to establish whether decay occurs by a step-by-step cascade or whether level-bypassing transitions are important.[15] In addition, the latter and the appearance of levels not predicted from the single-ion absorption spectrum may indicate transitions involving a pair of coupled ions.[16]

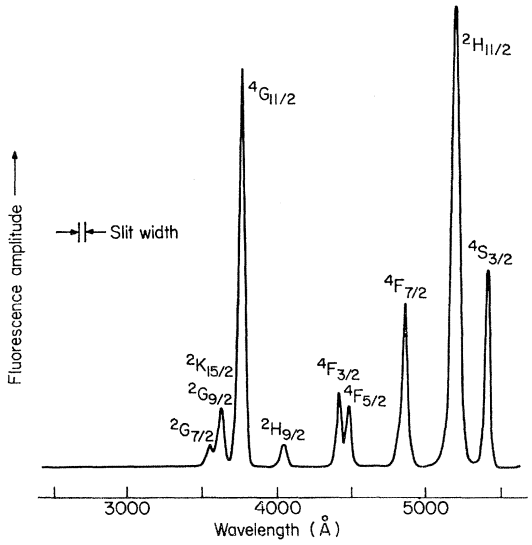

FIG. 8. Excitation spectrum of $^4S_{3/2}$ fluorescence at 78°K.

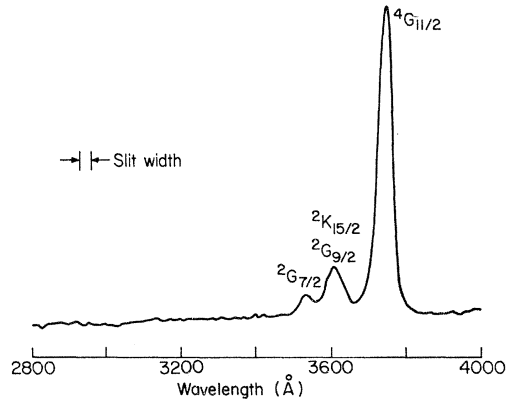

FIG. 9. Excitation spectrum of $^4G_{11/2}$ fluorescence at 78°K.

[13] H. H. Caspers, R. A. Buchanan, and H. R. Marlin, J. Chem. Phys. **41**, 94 (1964).

[14] W. M. Yen, W. C. Scott, and A. L. Schawlow, Phys. Rev. **136**, A271 (1964).

[15] F. Varsanyi, in *Quantum Electronics*, edited by P. Grivet and N. Bloembergen (Columbia University Press, New York, 1964), p. 787.

[16] F. Varsanyi and G. H. Dieke, Phys. Rev. Letters **7**, 442 (1961).

Examples of the types of excitation spectra expected from a multilevel system are seen by again considering the simple four-level system in Fig. 3(b). Assume radiation is continuously applied to excite ions into level 4 with a probability P proportional to the product of the absorption cross section and the pump intensity. The steady-state equilibrium populations are found by introducing P into Eq. (9) and equating the left-hand side to zero. The solutions for the usual experimental condition of weak pumping, $\tau_4 P \ll 1$, are

$$n_4 = \frac{\tau_4 P}{1+\tau_4 P} n_1 \approx \tau_4 P N ,$$

$$n_3 = \tau_3 w_{43} n_4 \approx \tau_3 \left(\frac{w_{43}}{W_4}\right) P N ,$$

$$n_2 \approx \tau_2 \left(\frac{w_{32}}{W_3}\frac{w_{43}}{W_4} + \frac{w_{42}}{W_4}\right) P N , \qquad (15)$$

where N is the total number of ions in the system. The intensity of level 4 in the excitation spectrum of level 3 is therefore proportional to the ratio of the probability for decay $4 \rightarrow 3$, w_{43}, to the total probability for decay from 4, W_4. Level 4 may appear in the excitation spectrum of level 2 either by a step-by-step cascade $4 \rightarrow 3 \rightarrow 2$ with intensity proportional to $(w_{43}/W_4) \times (w_{32}/W_3)$ or by direct transitions $4 \rightarrow 2$ proportional to (w_{42}/W_4). Since closely spaced levels decay predominantly by nonradiative cascade to a lower fluorescent level [characterized by $(w_{32}/W_3) \approx 1$, $(w_{43}/w_4) \approx 1$, and $w_{42} \approx 0$ in the present level system], the excitation spectrum of this level will reflect that of the corresponding absorption spectrum. If, however, a transition such as $3 \rightarrow 2$ is forbidden or weak, $w_{32} \approx 0$ and level 3 would not appear in the excitation spectrum of level 2. Because this would also bottleneck any energy cascade from higher levels, only those higher levels appear which have additional decay modes to level 2 via transitions which bypass level 3.

The rates of nonradiative transitions can be determined from excitation spectra. As an example, the intensities of lines originating from levels 2, 3, 4 in the excitation spectrum of level 2 are proportional to their integrated absorption cross sections multiplied by 1, (w_{32}/W_3), and $(w_{32}w_{43}/W_3W_4 + w_{42}/W_4)$, respectively. These factors are a measure of the fraction of ions cascading in various decay modes and by comparing the relative intensities of corresponding lines in the excitation spectrum with independent measurements of the absorption cross sections, they can be determined. Because level 2 is populated both by level-by-level cascade via w_{43} and w_{32} and by direct transitions via w_{42}, additional measurements of the excitation spectrum of level 3 are needed to find the ratio w_{43}/W_4. Combining these results with lifetime measurements of W_k^{-1} yields the probabilities w_{ij}.

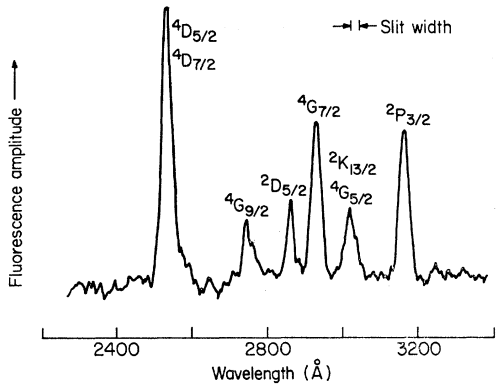

FIG. 10. Excitation spectrum of $^2P_{3/2}$ fluorescence at 78°K.

Observations

Excitation spectra were recorded for all fluorescent levels of Er^{3+} in LaF_3 except $^4I_{13/2}$; the spectra for $^4I_{11/2}$, $^4F_{9/2}$, $^4S_{3/2}$, $^4G_{11/2}$, and $^2P_{3/2}$ for a sample containing 0.095% Er are shown in Figs. 7–11. (The results as shown are uncorrected for the intensity variation of the incident radiation arising from the spectral distribution of the source, a xenon arc lamp, and the grating efficiency of the monochromator, 3000 Å blaze.) All levels up to and including $^2G_{7/2}$ which are expected from the absorption spectrum are observed in the excitation spectra of lower fluorescing levels. Both level-by-level cascade and radiative transitions which bypass

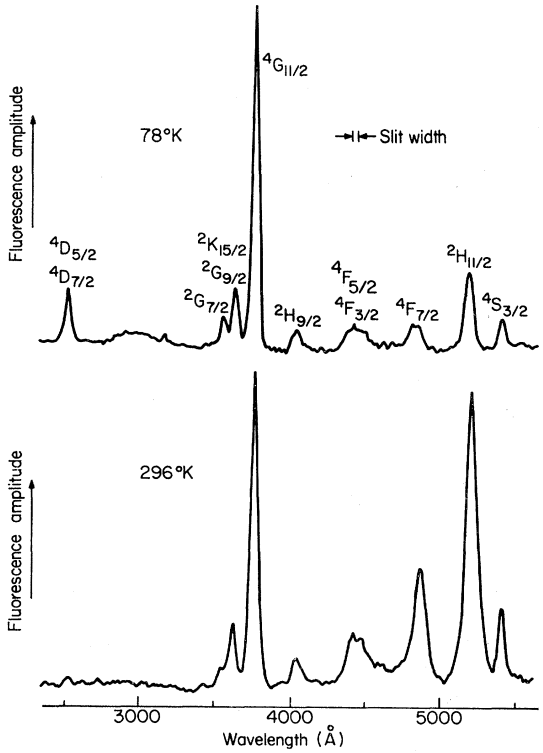

FIG. 11. Excitation spectrum of $^4F_{9/2}$ fluorescence at two different temperatures.

TABLE II. Relative intensities of lines in the absorption and excitation spectrum of $LaF_3:Er^{3+}$ (normalized with respect to $^2H_{11/2}$).

Excited level	Absorption spectrum (77°K)	Excitation spectrum at 77°K $^4S_{3/2}$	Excitation spectrum at 77°K $^4I_{11/2}$	Excitation spectrum at 500°K $^4S_{3/2}$	Excitation spectrum at 500°K $^4I_{11/2}$
$^4S_{3/2}$	0.28	0.31	0.33	0.17	0.15
$^2H_{11/2}$	1.00	1.00	1.00	1.00	1.00
$^4F_{7/2}$	0.26	0.25	0.24	0.30	0.30
$^4F_{5/2}$, $^4F_{3/2}$	0.2	0.19	0.20	0.14	0.13
$^2H_{9/2}$	0.12	0.06	0.10	0.06	0.07
$^4G_{11/2}$	2.01	0.90	1.21	0.72	0.99

levels are active in the energy decay. No evidence of virtual levels or missing levels, such as reported[15] for Er^{3+} in $LaCl_3$, was observed, thereby indicating again that decay by energy transfer arising from ion-ion coupling is not important in the crystals used.

The relative intensities of levels $^4S_{3/2}$ through $^2G_{7/2}$ which are common to the excitation spectra of $^4I_{11/2}$ and $^4S_{3/2}$ are compared in Table II. (The results were corrected for the spectral variation of the incident radiation and normalized to $^2H_{11/2}$.) The relative intensities of levels $^4S_{3/2}$ through $^4F_{3/2}$ are equal, within experimental error, in the two spectra. In this region the energy levels are separated by <1600 cm^{-1} and rapid level-by-level nonradiative cascade occurs. The intensities of the higher levels $^2H_{9/2}$ and $^4G_{11/2}$, however, are not equal in the two spectra. In addition to cascade $^4G_{11/2} \rightarrow {}^2H_{9/2} \rightarrow {}^4F_{3/2} \cdots {}^4S_{3/2}$, these levels decay by emission to $^4F_{9/2}$ and levels of the ^4I ground term. This direct decay bypasses $^4S_{3/2}$ and therefore $^4G_{11/2}$ and $^2H_{9/2}$ are more important in the excitation spectrum for $^4I_{11/2}$ than for $^4S_{3/2}$ at 77°K. Note that at 500°K, the intensity of $^2H_{9/2}$ is more nearly equal in the two spectra, indicating a thermal enhancement of the $^2H_{9/2} \rightarrow {}^4F_{3/2}$ decay.

The relative intensities of the J multiplets observed in the absorption spectrum at 77°K are also included in Table II. The similar intensities observed for $^4S_{3/2}$ through $^4F_{3/2}$ demonstrates decay via a nonradiative cascade to $^4S_{3/2}$. As expected, the intensities of $^2H_{9/2}$ and $^4G_{11/2}$ are smaller in the two excitation spectra because several radiative transitions from these levels occur which do not contribute to the excitation of either the $^4S_{3/2}$ or $^4I_{11/2}$ fluorescence.

As discussed later and in II, the rate of nonradiative decay by multiphonon emission is very dependent upon the proximity of other energy levels.[17] Because of the comparatively large energy gap from $^2P_{3/2}$ to $^2G_{7/2}$, the probability for $^2P_{3/2} \rightarrow {}^2G_{7/2}$ decay is small and therefore acts as a bottleneck for energy cascade. This is also suggested by the fact that the $^2P_{3/2}$ lifetime is two orders of magnitude longer than that of $^4G_{11/2}$ at 77°K and therefore will limit any population buildup and fluorescence from $^4G_{11/2}$ when ions are initially excited into $^2P_{3/2}$. The $^2P_{3/2}$ and higher excited states which are seen in the excitation spectrum of $^2P_{3/2}$ in Fig. 10 are absent or are observed only very weakly in the excitation spectra of lower levels. The weak appearance of levels $^2P_{3/2}$ through $^4G_{9/2}$ and $^4D_{5/2}$-$^4D_{7/2}$ in the $^4I_{11/2}$ and $^4F_{9/2}$ excitation spectra (observed under conditions more favorable than used in recording Figs. 7 and 11) is due, at least in part, to direct radiative transitions from $^2P_{3/2}$ and $^4D_{5/2}$ rather than solely by cascade via $^2P_{3/2}$ and intervening levels. This was confirmed by pulsed selective excitation experiments in which the rise time is indicative of the initial or limiting lifetime in the decay to the fluorescing level. The $^4D_{5/2}$-$^4D_{7/2}$ peak in the spectrum of $^4F_{9/2}$ at 77°K arises, as shown in II, principally from the large radiative probability for $^4D_{5/2} \rightarrow {}^4F_{9/2}$.

With increasing temperature, stimulated phonon emission between adjacent levels increases and thereby accounts for a greater fraction of the decay at the expense of competing radiative transitions. This is observed in the case of the $^4D_{5/2}$-$^4D_{7/2}$ peak in the $^4F_{9/2}$ excitation spectrum discussed above. At higher temperatures, more excited ions in $^4D_{5/2}$ decay to $^4G_{9/2}$ and via cascade become bottlenecked at $^2P_{3/2}$. The $^4D_{5/2}$-$^4D_{7/2}$ levels thus become less effective for $^4F_{9/2}$ fluorescence excitation. The decreased lifetime of $^4D_{5/2}$ at higher temperatures reflects the increased probability for decay. The change in relative intensities of the $^4G_{11/2}$-$^2H_{9/2}$ and $^4F_{3/2}$-$^3S_{3/2}$ groups of excitation levels with temperature (see Figs. 5 and 11) can be explained similarly.

CONCLUSIONS

An analysis of the time-dependent fluorescence properties following pulsed selective excitation and steady-state excitation and fluorescence spectra demonstrates that the decay modes of a multilevel system such as Er^{3+} can be complex even in the absence of ion-ion transfer. Energy decay by step-by-step nonradiative cascade between closely spaced levels and large level-bypassing transitions are both active. Enhancement of nonradiative processes with increased temperature is evident from changes in the excitation spectra, transient fluorescence behavior, and decreased excited state lifetimes. No virtual levels or unusual gaps or intensities were observed in the excitation spectra thereby indicating that resonant energy transfer was not important in determining the lifetimes in the $LaF_3:Er^{3+}$ crystals used. From the information about fluorescing levels, excitation modes, and lifetimes in Table I, the modes of energy cascade, important bottlenecks, and levels useful for laser or quantum counter-action can be deduced.

The rate of energy cascade and the existence of critical bottlenecks are dependent upon the probabilities for radiative transitions and, in the case of multi-

[17] A. Kiel, in *Quantum Electronics*, edited by P. Grivet and N. Bloembergen (Columbia University Press, New York, 1964), p. 765.

phonon emission, the size of the energy gap, the character of the eigenstates, and the vibrational properties of the host lattice.[18] There is a general trend throughout the energy level scheme of $LaF_3:Er^{3+}$ of shorter lifetimes as the energy gap to the next-lower level decreases[19] or as the number of possible fluorescence transitions increases. This is seen in Table III where the lifetimes of several levels at liquid-nitrogen temperatures are compared with the minimum energy gap to the highest crystal-field level of the next-lower $[SLJ]$ multiplet. The temperature dependences of the fluorescence lifetimes exhibit a somewhat similar trend, namely, the smaller the energy gap to the next lower level, the sooner the lifetime begins to decrease with increasing temperature; however, in some cases thermal population of faster relaxing states must also be considered.

Whereas the modes of decay and excited-state lifetimes for Er^{3+} in LaF_3 have been established, the rates and relative importance of radiative and nonradiative transitions from a given level remain to be determined. This is treated in II where the probabilities for radiative decay of various multipole nature are calculated and compared with fluorescence intensities and observed lifetimes to determine the nonradiative relaxation contributions.

TABLE III. Comparison of the lifetime and energy gap to the next lower J multiplet for several levels of $LaF_3:Er^{3+}$.

Level	Energy gap (cm^{-1})	Lifetime (msec)	Level	Energy gap (cm^{-1})	Lifetime (μsec)
$^4I_{13/2}$	6160	13	$^4F_{5/2}$	1610	$\lesssim 10$
$^4I_{11/2}$	3480	11	$^2H_{9/2}$	1860	95
$^4I_{9/2}$	2020	~ 0.15	$^4G_{11/2}$	1640	~ 3
$^4F_{9/2}$	2700	0.75	$^2P_{3/2}$	3320	290
$^4S_{3/2}$	3030	1.0	$^4D_{5/2}$	2000	20

ACKNOWLEDGMENT

The experimental assistance of P. Kocincki during the the course of this investigation is very gratefully acknowledged.

[18] An example of the restrictions imposed by selection rules upon the number of possible radiative and nonradiative transitions is seen in the case of the relaxation of Eu^{3+} in LaF_3. See M. J. Weber, in Proceedings of the Johns Hopkins Conference on Optical Properties of Ions in Crystals (to be published).

[19] A similar correlation has been noted by Barasch and Dieke (Ref. 4) for the lifetimes of Er^{3+} levels in various chlorides.

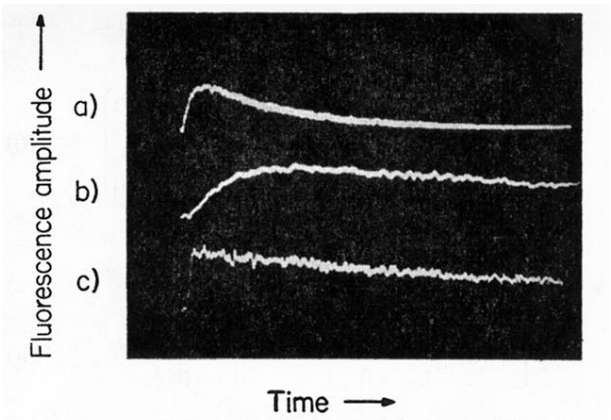

FIG. 4. Oscilloscope photograph of $^4S_{3/2}$ fluorescence at 77°K following pulsed excitation into (a) $^4G_{11/2}$, total sweep 5.0 msec, (b) $^4G_{11/2}$, total sweep 1.0 msec, (c) $^2H_{11/2}$, total sweep 1.0 msec.